Available online at www.sciencedirect.com

SciVerse ScienceDirect

Procedia Engineering 36 (2012) 121 – 127

Procedia Engineering

www.elsevier.com/locate/procedia

IUMRS-ICA 2011

Ultrastructural Observation of Hydroxyapatite Ceramics with Preferred Orientation to a-plane Using High-resolution Transmission Electron Microscopy

Zhi Zhuang[a], Takuya Miki[a], Midori Yumoto[a], Toshiisa Konishi[b], Mamoru Aizawa[a,b]*

[a]*Department of Applied Chemistry, School of Science and Technology, Meiji University, 1-1-1 Higashimita, Tama-ku, Kawasaki, 214-8571, Japan*

[b]*Kanagawa Academy of Science and Technology (KAST), KSP East 404, 3-2-1 Sakado, Takatsuku, Kawasaki,213-0012, Japan*

Abstract

The dense hydroxyapatite (HAp) ceramics with preferred orientation to *a*-plane were fabricated using composite powders of single-crystal apatite fibers (AF) and wet-synthesized apatite gels (AG). AF was synthesized by homogeneous precipitation method. The composites of AF and AG were prepared as the following process. Aqueous $(NH_4)_2HPO_4$ solutions were added into the AF slurry with the amount of 1 mass%. In addition, aqueous $Ca(NO_3)_2$ solutions were added dropwise to the slurry to precipitate the AG on the AF at room temperature, and then aged at room temperature for 24 h with stirring. The dried powders were uniaxially pressed at 200 MPa of compaction pressure and then fired at 1300 ºC for 5 h. All the resulting ceramics were identified with HAp single phases. The (100), (200) and (300) reflections which correspond to *a*-plane were more intense than those of a standard HAp ceramics. With increasing the additive amount of AG, the orientation degree of *a*-plane decreased, and the relative density increased. Furthermore, the ultrastructure of the resulting ceramics was examined by high-resolution transmission electron microscopy. The selected area electron diffraction patterns showed clear spots corresponding to [1$\underline{1}$0] zone axis direction of HAp crystal with high crystallinity. The lattice spacings of crystal grains were determined to be 0.34 nm or 0.68 nm which corresponds to the lattice constant of (002) or (001) plane of HAp crystal. Therefore, the resulting ceramics were HAp single phases with preferred orientation to *a*-plane.

© 2011 Published by Elsevier Ltd. Selection and/or peer-review under responsibility of MRS-Taiwan
Open access under CC BY-NC-ND license.

Keywords: Hydroxyapatite ceramics; preferred orientation; microstructure; high-resolution transmission electron microscopy

* Corresponding author. Tel.: +81-44-934-7237; Fax: +81-44-934-7906.
E-mail address: mamorua@isc.meiji.ac.jp

1877-7058 © 2012 Published by Elsevier Ltd. Open access under CC BY-NC-ND license.
doi:10.1016/j.proeng.2012.03.019

1. Introduction

Hydroxyapatite ($Ca_{10}(PO_4)_6(OH)_2$; HAp) is an inorganic compound which is close to chemical compositions of human hard tissues, and it has good biocompatibility and bioactivity. Synthetic HAp is widely used as an adsorbent of bio-related substances and a raw material for artificial bones and teeth [1, 2]. The HAp crystal belongs to hexagonal system, its unit cell parameters are $a = b = 0.943$ nm and $c = 0.688$ nm, and there are two types of crystal planes: $a(b)$-planes and c-planes [3]. The $a(b)$-planes are rich in calcium ions and charged on positive; the c-planes rich in phosphate ions or hydroxide ions and charged on negative. Actually, the HAp crystals in a cortical bone and dental enamel have preferred orientation to the c- and $a(b)$-axis directions, respectively.

By controlling the morphology of HAp crystals, novel properties may be produced by enabling controlled orientation of crystal planes. Actually, in previous study, we have successfully synthesized a single-crystal apatite fiber (AF) [4]. The ultrastructure of AF was examined by using high-resolution transmission electron microscopy (HR-TEM), the results indicated that the AF particle was highly strained single crystal with the c-axis orientation parallel to the long axis of the fiber [5]. We have developed the high performance biomaterials using the AF. Utilizing the positive surface charge of these fibers, protein adsorption measurements were carried out. Thus, we found that the apatite fiber adsorbed the acidic proteins rather than the basic proteins [6]. Utilizing the fiber shape, we fabricated the porous ceramics with well-controlled pore size [7, 8] and then developed the hybrid materials having mechanical property similar to that of cortical bone [9, 10]. In addition, by utilizing the surface charge and fiber shape, the scaffold for tissue engineering were developed [11, 12].

In this work, the dense HAp ceramics with preferred orientation to a-plane were fabricated using the composite powders of AF and wet-synthesized hyrdroxyapatite gels (AG). The crystalline phase and microstructure of the resulting HAp ceramics with preferred orientation to a-plane were examined using powder X-ray diffraction (XRD), scanning electron microscope (SEM) and HR-TEM.

2. Experimental

2.1. Fabrication of the HAp ceramics with preferred orientation to a-plane

The AF powder was synthesized from the aqueous solution containing 0.167 mol·dm^{-3} $Ca(NO_3)_2$, 0.100 mol·dm^{-3} $(NH_4)_2HPO_4$, 0.50 mol·dm^{-3} $(NH_2)_2CO$ and 0.1 mol·dm^{-3} HNO_3. The starting solution of 750 cm^3 was refluxed at 80 ºC for 24 h, for another 72 h refluxed at 90 ºC. The AF with the amount of 30 mass% (AG30%AF) and 50 mass% AG (AG50%AF) were prepared as the following process. Aqueous $(NH_4)_2HPO_4$ solutions were added into the AF slurry with the amount of 1 mass%. In addition, aqueous $Ca(NO_3)_2$ solutions were added dropwise to the slurry to precipitate the AG on the AF at room temperature, and then aged at room temperature for 24 h with stirring. The powders of AF, AG30%AF and AG50%AF were filtrated and dried with oven at 110 ºC for 1 day. About 0.8 g of dried powders were uniaxially pressed at 200 MPa of compaction pressure and then fired at 1300 ºC for 5 h in air atmosphere using tube type electric furnace.

2.2. Characterizations of starting powders and resulting ceramics

The crystalline phases of starting powders and resulting ceramics were identified by XRD (MiniFlex, Rigaku) using Cu-K_α radiation generated at 30 kV and 15 mA. Those particle morphologies and surface structures were observed by SEM (JSM6390LA, JEOL). Furthermore, those ultrastructures were examined by HR-TEM (JEM-2100F, JEOL) instrument at an accelerated voltage of 200 kV. HR-TEM

samples of resulting ceramics were thinned by Ar gas irradiation treatment using ion slicer (EM-09100IS, JEOL) and coated with carbon.

3. Results and Discussion

Figure 1(a, b, c) shows the XRD patterns of the AF (Fig. 1(a)), AG30%AF (Fig. 1(b)) and AG50%AF (Fig. 1(c)) powders. All the resulting powders were identified with HAp single phase, and the (100), (200) and (300) reflections which were proper for *a*-plane of HAp, were specifically developed. This result indicates that those HAp powders have preferred orientation in the *c*-axis direction of the hexagonal crystal, leading to develop the *a*-plane of the HAp crystal. The XRD patterns of the resulting ceramics were shown in Fig. 1(d, e, f). The crystalline phase of the resulting ceramics kept HAp phase and the preferred orientation to *a*-plane.

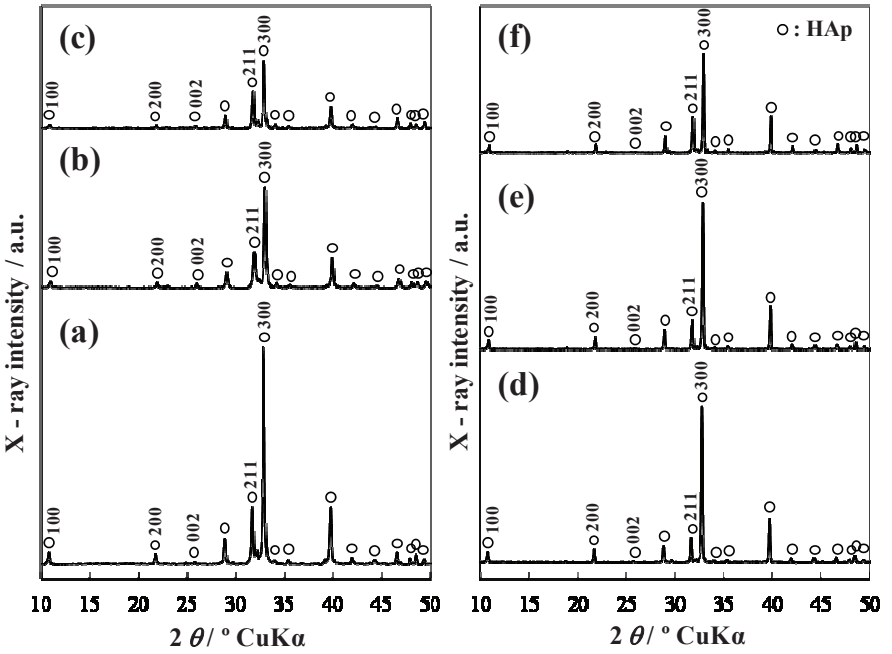

Fig. 1 XRD patterns of the starting powders and the resulting ceramics: (a) AF powder, (b) AG30%AF powder, (c) AG50%AF powder, (d) AF ceramics, (e) AG30%AF ceramics and (f) AG50%AF ceramics.

The orientation degree of *a*-plane of each ceramic was calculated on the basis of the intensities of (300), (211) and (002) reflections according to Eq. 1. The orientation degree was in order of AF ceramics (86.0%) > AG30%AF ceramics (82.5%) > AG50%AF ceramics (72.4%). This result suggests that the orientation degree of ceramics was decreased with increasing the additive amount of AG.

$$\text{Orientation degree of } a\text{-plane} = I_{(300)} / (I_{(300)} + I_{(211)} + I_{(002)}) \times 100\% \ \ldots \text{(Eq. 1)}$$

Figure 2(a, b, c) shows the SEM micrographs of starting powders. In Fig. 2(a), AF was composed of fiber-shaped particles which had smooth surfaces. For AG30%AF powder (Fig. 2(b)), most of

precipitated AG particles adhered on the surface of AF particles. However, in the case of AG50%AF powder (Fig. 2(c)), the AG particles also existed as agglomerates in the composite powder, together with the AF coated with AG. Fig. 2(d, e, f) shows the SEM micrographs of the resulting ceramics. In all the resulting ceramics, the shape of the AF particle partly was maintained. In addition, with the additive amount of AG was increased, the number of pores was decreased.

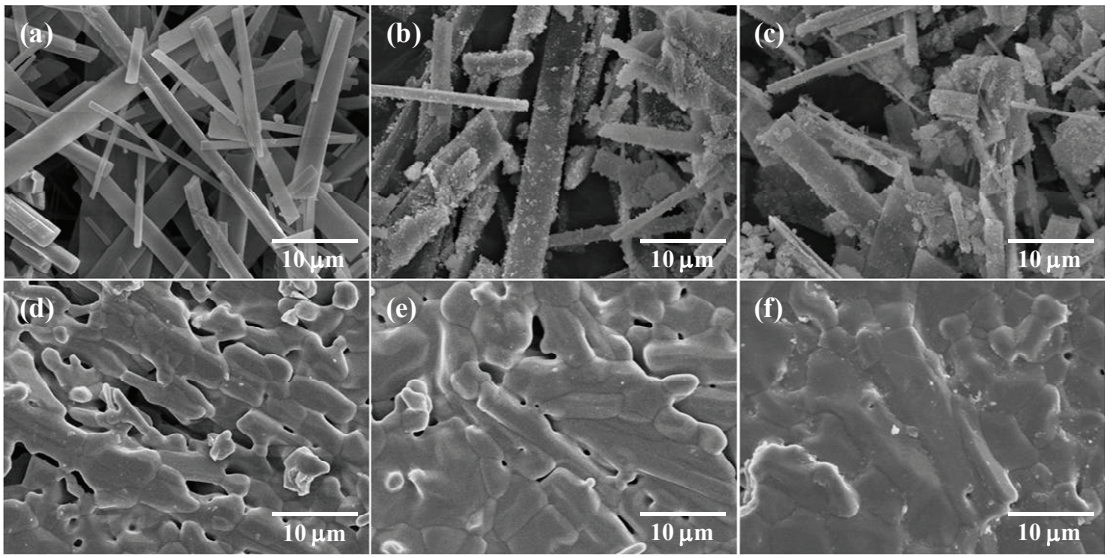

Fig. 2 SEM micrographs of the starting powders and the resulting ceramics: (a) AF powder, (b) AG30%AF powder, (c) AG50%AF powder, (d) AF ceramics, (e) AG30%AF ceramics and (f) AG50%AF ceramics.

The relative density of the resulting ceramics was determined by Eq. 2. The order inverted as follows: AG50%AF ceramics (88.8%) > AG30%AF ceramics (85.6%) > AF ceramics (77.9%). This result accorded as result of SEM observation.

$$\text{Relative density} = \text{Bulk density} / (3.16\ \text{g}\cdot\text{cm}^{-3}) \times 100\% \ \ldots \ (\text{Eq. 2})$$

Figure 3(a~e) shows HR-TEM micrographs (Fig. 3(a, c, d)), selected area electron diffraction (SAED) patterns (Fig. 3(b)) and fast fourier transform (FFT) patterns (Fig. 3(e)) of AF powder. Figure 3(a) showed a low-magnification TEM image of an AF particle. SAED observations were performed at several areas along long-axis of the fiber. All the SAED patterns had a similar geometry as shown in Fig. 3(b). From these SAED patterns, clear spots which arranged in rectangles could be observed, and the spots aligned along long-axis of the fiber were confirmed as (00*l*) spots.

Middle-magnification HR-TEM lattice image of AF particle was shown in Fig. 3(c). The lattice spacings along long-axis and short-axis of the fiber were determined to be 0.34 nm and 0.47 nm which corresponded to the lattice constants of (002) plane and (110) plane of HAp crystal, respectively. Therefore, the direction paralleled along long-axis of the fiber was *c*-axis direction, its vertical direction was *a*-axis direction, and the observed direction was the [1$\underline{1}$0] zone axis.

The high-magnification HR-TEM lattice image and the corresponding FFT pattern of AF particle were shown in Fig. 3(d) and (e). From this lattice image, a highly periodic sequence of atom can be observed.

The white rectangle of insert in Fig. 3(d) with 0.68 nm high and 0.94 nm long, corresponded to a unit cell of HAp crystal which observed from *a*-plane direction. The corresponding FFT pattern (Fig. 3(e)) also showed highly-orientated spots as same as the SAED pattern (Fig. 3(b)). These results indicated that the AF was high crystalline HAp single-crystal with preferred orientation to *c*-axis direction.

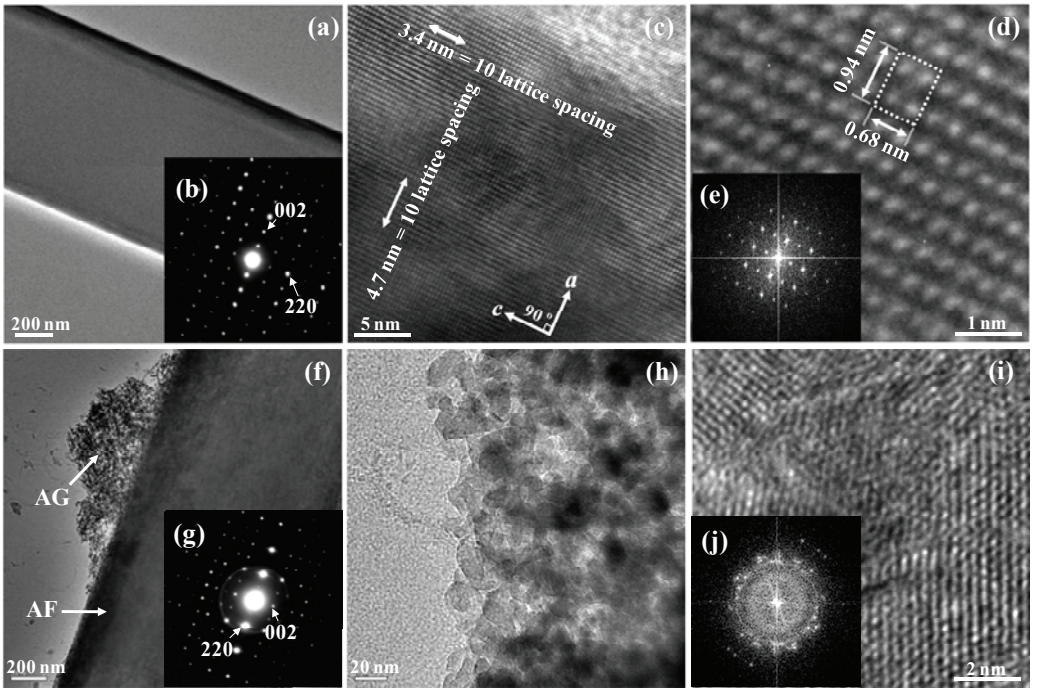

Fig. 3 HR-TEM micrographs, SAED patterns and FFT patterns of AF and AG30%AF powders: (a) Low-magnification TEM micrograph of AF powder, (b) SAED pattern of AF powder, (c) middle-magnification HR-TEM micrograph of AF powder, (d) high-magnification HR-TEM micrograph of AF powder, (e) FFT pattern of AF powder, (f) low-magnification HR-TEM micrograph of AG30%AF powder, (g) SAED pattern of AG30%AF powder, (h) middle-magnification HR-TEM micrograph of AG30%AF powder, (i) high-magnification HR-TEM micrograph of AG30%AF powder and (j) FFT pattern of AG30%AF powder.

The ultrastructure observation results of AG30%AF powder were shown in Fig. 3(f~j). From low-magnification TEM image (Fig. 3(f)), agglomerated AG particles which adhered on the surface of AF particle could be observed. The SAED pattern (Fig. 3(g)) shows clear spots according with single-crystal and Debye rings according with polycrystalline. In order to the diffraction spots shown the same geometry as that of AF, the Debye rings could be confirmed as the diffractions resulting from the AG particles.

The middle-magnification HR-TEM image of AG particles was shown in Fig. 3(h). The primary particles of AG were ~20-40 nm in length and ~10-30 nm in width.

Figure 3(i and j) showed the high-magnification HR-TEM image of one AG crystal and the corresponding FFT pattern. The direction of crystal lattice was random and the FFT pattern showed Debye rings. Therefore, the AG particle was polycrystalline with isotropic orientation.

The HR-TEM images and SAED patterns of AG30%AF ceramics were shown in Fig. 4. In Fig. 4(a), we can observe three crystal grains (#1, #2 and #3). The SAED pattern from crystal grain #1 (Fig. 4(b)) showed clear spots corresponding to *a*-plane of HAp crystal structure with high crystallinity. The SAED

patterns of grain #2 and #3 also revealed a similar geometry as that of grain #1. The lattice images were shown in Fig. 4(c). The 10 lattice spacings of each crystal grain were determined to be #1=6.6 nm, #2=3.4 nm and #3=0.32 nm. Therefore, one lattice spacing was #1=0.66 nm, #2=0.34 nm and #3=0.32 nm, respectively. These values closely accorded with the lattice parameters of *c*-axis ($d_{(001)}$=0.68 nm and $d_{(002)}$=0.34 nm) in the HAp crystal. Therefore, the resulting HAp ceramics kept the preferred orientated in the *c*-axis direction.

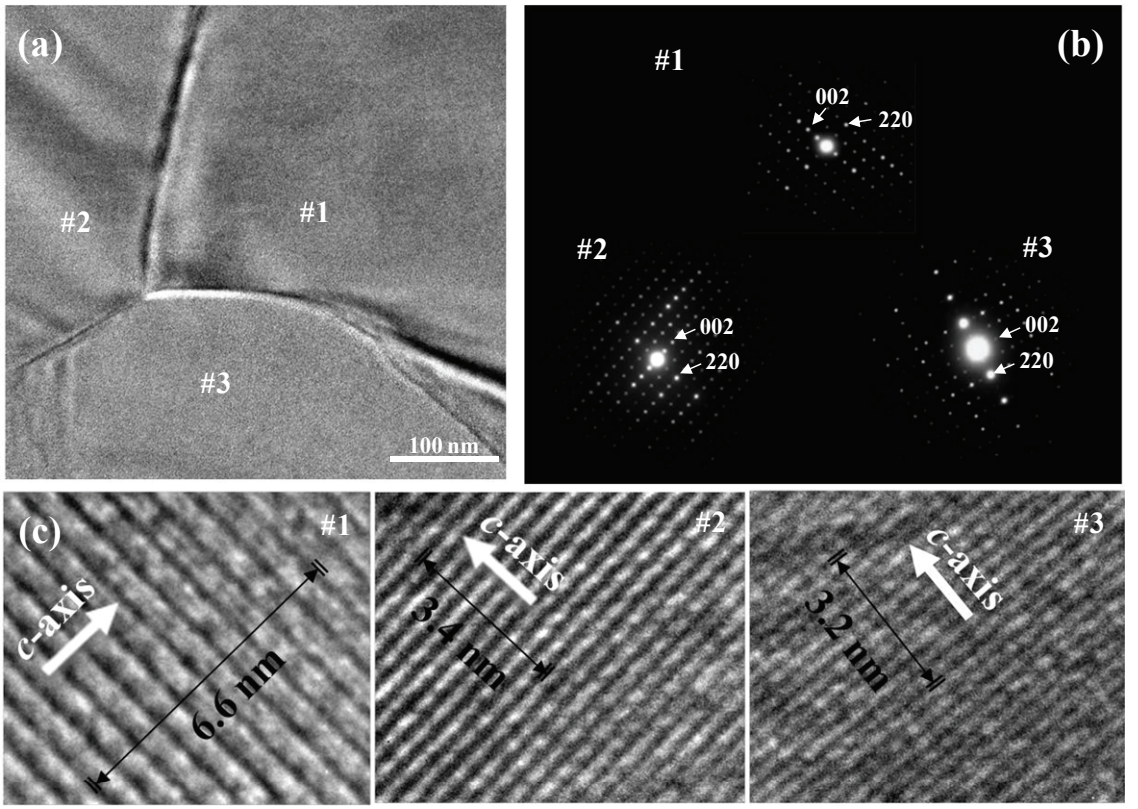

Fig. 4 HR-TEM micrographs and SAED patterns of AG30%AF ceramics: (a) Low-magnification TEM micrograph of AG30%AF ceramics, (b) SAED patterns of crystal grains #1, #2 and #3, (c) high-magnification HR-TEM micrographs of crystal grains #1, #2 and #3.

4. Conclusions

The HAp ceramics with preferred orientation to *a*-plane were fabricated using composite powders of AF and AG. The crystalline phases and microstructures of starting powders and resulting ceramics were examined by XRD, SEM and HR-TEM. The AF particles were highly strained single crystal with the *c*-axis orientation parallel to the long axis of the fiber, and the AG particles were polycrystalline with isotropic orientation. All the resulting ceramics were identified with HAp single phases, and the (100), (200) and (300) reflections which correspond to the *a*-plane were more intense than those of a standard HAp ceramics. In addition, with the additive amount of AG increased, the orientation degree of *a*-plane

decreased, and the relative density increased. Furthermore, the results of SAED patterns and lattice images suggest that the resulting ceramics kept the preferred orientated in the *c*-axis direction.

References

[1] Hench LL, *J Am Ceram Soc* 1991; **74**:1487-510.
[2] Kawasaki T, Takahashi S, Ikeda K, *Eur J Biochem* 1985; **152:361**-7.
[3] Kay MI, Young RA, Posner AS, *Nature* 1964; **204:1050**-2.
[4] Aizawa M, Ueno H, Itatani K, Okada I, *J Eur Ceram Soc*, 2006; **26**:501-7.
[5] Aizawa M, Porter AE, Best SM, Bonfield W, *Biomaterials* 2005; **26**:3427-33.
[6] Zhuang Z, Aizawa M, *Arch BioCeram Res* 2010; **10:153**-6.
[7] Aizawa M, Howell FS, Itatani K, Yokogawa Y, Nishizawa K, Toriyama M, Kameyama T, *J Ceram Soc Jpn* 2000; **108**:249-53.
[8] Kawata M, Uchida H, Itatani K, Okada I, Koda S, Aizawa M, *J Mater Sci: Mater Med* 2004; **15**:817-23.
[9] Yoshimi T, Sugiyama N, Takeoka Y, Rikukawa M, Oribe K, Aizawa M, *J Ceram Soc Austr* 2010; **47**:18-22.
[10] Shigemitsu Y, Sugiyama N, Oribe K, Rikukawa M, Aizawa M, *J Ceram Soc Jpn* 2010; **118**:1181-7.
[11] Honda M, Fujimi TJ, Izumi S, Izawa K, Aizawa M, Morisue H, Tsuchiya T, Kanzawa N, *J Biomed Mater Res* 2010; **94**:937-44.
[12] Aizawa M, Shinoda H, Uchida H, Okada I, Fujimi TJ, Kanzawa N, Morisue H, Matsumoto M, Toyama Y, *Phosphorus Res Bull* 2004; **17**:268-73.